Copyright © 2017 Tech Science Press CMES, vol.113, no.2, pp.219-237, 2017

Local and biglobal linear stability analysis of parallel shear flows

Sanjay Mittal[1] **and Anubhav Dwivedi** [1]

Abstract: Linear Stability Analysis (LSA) of parallel shear flows, v ia local and global approaches, is presented. The local analysis is carried out by solving the Orr-Sommerfeld (OS) equation using a spectral-collocation method based on Chebyshev polynomials. A stabilized finite element formulation is employed to carry out the global analysis using the linearized disturbance equations in primitive variables. The local and global analysis are compared. As per the Squires theorem, the two-dimensional disturbance has the largest growth rate. Therefore, only two-dimensional disturbances are considered. By its very nature, the local analysis assumes the disturbance field to be spatially periodic in the streamwise direction. The global analysis permits a more general disturbance. However, to enable a comparison with the local analysis, periodic boundary conditions, at the inlet and exit of the domain, are imposed on the disturbance. Computations are carried out for the LSA of the Plane Poiseuille Flow (PPF). The relationship between the wavenumber, α, of the disturbance and the streamwise extent of the domain, L, in the global analysis is explored for $Re = 7000$. It is found that α and L are related by $L = 2\pi n/\alpha$, where n is the number of cells of the instability along the streamwise direction within the domain length, L. The procedure to interpret the results from the global analysis, for comparison with local analysis, is described.

Keywords: Linear stability analysis; local analysis; plane Poiseuille flow; Orr-Sommerfeld equation; global analysis

1 Introduction

The hydrodynamic stability of laminar flows has received significant attention and has been investigated by several researchers in the past [Schmid and Henningson (2001); Chandrasekhar (1981);Huerre and Monkewitz (1990);Huerre (2000); Chomaz (2005)]. The linear stability of parallel shear flows can be analyzed via

[1] Department of Aerospace Engineering, Indian Institute of Technology Kanpur, UP 208016, India
[2] E-mail: smittal@iitk.ac.in

finding solution to the Orr-Sommerfeld (OS) equation [Orr (1907); Sommerfeld (1908)], with suitable boundary conditions. The disturbance field is assumed to be a plane wave whose amplitude varies transverse to the flow and is periodic in the homogeneous directions. The analysis can be carried out in either a spatial or temporal framework [Boiko, Dovgal, Grek, and Kozlov (2012)]. The spatial analysis assumes that the disturbance field develops in space. The spatial growth rate is determined for different values of frequency and Reynolds number. In contrast, the temporal analysis assumes that the disturbance develops in time. As per the Squire's theorem [Schmid and Henningson (2001)], the 2D disturbance is the most critical in terms of its growth rate. Therefore, it is sufficient to consider two-dimensional disturbances that have streamwise periodicity [Boiko, Dovgal, Grek, and Kozlov (2012)]. The analysis is carried out to determine temporal growth rate at various *Re* and for disturbances with different values of streamwise wavenumber. The spatial and temporal approaches for local analysis are related to each other [Huerre (2000)]. For example, Gaster (1962) proposed a transformation for that, approximately, relates the temporal and spatial growth. Several methods have been used to solve the OS equations. Davey and Drazin (1969) utilized Bessel functions to represent the disturbance field and analyze the stability of pipe Poiseuille flow. Orszag (1971) used Chebyshev polynomials to solve the OS equation for the plane Poiseuille flow. Saraph, Vasudeva, and Panikar (1979) used Galerkin's weighted residual method to carry out the stability analysis of plane Poiseuille flow and magneto-hydrodynamic flows. Garg and Rouleau (1972) used asymptotic analysis to carry out the linear stability analysis in pipe flow. The method has also been applied, in a local sense, to spatially developing flows [Pierrehumbert (1985); Yang and Zebib (1989); Monkewitz (1988); Chomaz, Huerre, and Redekopp (1988)]. In this approach, the flow profiles at different streamwise stations are analyzed by assuming that each profile corresponds to an independent parallel flow. The local analysis, at each streamwise station of the flow, involves solving the OS equation, with suitable boundary conditions.

An alternate approach to investigate the linear stability of fluid flows is the BiGlobal and TriGlobal stability analysis [Theofilis (2011); Swaminathan, Sahu, Sameen, and Govindrajan (2011)]. Unlike in the local analysis, in this approach the disturbance field is represented globally, including in the streamwise direction. The analysis results in global modes which, depending on the sign of the growth rate, may either grow or decay in the entire computational domain with time. The global analysis is usually much more computationally expensive than the local one. Such an approach has been used to analyze the global linear stability properties of several non-parallel flows [Mittal (2004); Chomaz (2005); Schmid and Henningson (2001)]. Swaminathan, Sahu, Sameen, and Govindrajan (2011) carried out a global linear stability analysis of a diverging channel flow using spectral collocation method. Mittal and Kumar (2003) used a stabilized finite element method for the global LSA of stationary and rotating cylinder. Later, Verma and Mittal (2011) used a similar approach for carrying out global LSA to investigate the existence and stability of secondary wake mode of a two-dimensional flow past a circular cylinder. More recently, Navrose, Meena, and Mittal (2015) carried out LSA of spinning cylinder in a uniform flow and identified several unstable three-dimensional modes for various rotation rates of the spinning cylinder.

In the present work, Linear Stability Analysis (LSA) of the plane Poiseuille flow is carried out. Local and global analyses are considered. The solutions to the OS equation for local analysis have been obtained in a temporal framework. A spectral collocation method based on Chebyshev polynomials [Schmid and Henningson (2001)] is used to solve the governing Orr-Sommerfeld (OS) equation. The global LSA of the plane Poiseuille flow is carried out using a stabilized finite element formulation. The governing equations are cast in the primitive variables: velocity and pressure. Equal-order finite-element interpolation functions are used for pressure and velocity disturbance fields. Four-noded quadrilateral elements with bilinear interpolation is employed. The streamline-upwind/Petrov-Galerkin (SUPG) [Brooks and Hughes (1982)] and pressure-stabilizing/Petrov-Galerkin (PSPG) stabilization techniques [Tezduyar, Mittal, Ray, and Shih (1992)] are employed to stabilize the computations against spurious numerical oscillations. The finite element formulation results in a generalized eigenvalue-vector problem which is solved using the subspace iteration method [Stewart (1975)]. For carrying out the global analysis, we assume periodic boundary conditions at the inflow and the outflow for the disturbance field. This allows a direct comparison of the global LSA with the OS equation. A comparison between the local and global analysis of the plane Poiseuille flow at $Re = 7000$ is presented and is utilized to show the connection between the two analyses.

2 Governing Equations

2.1 Linearized Disturbance Equations

Let, $\Omega \subset \mathbb{R}^{n_{sd}}$ and $(0,T)$ be the spatial and temporal domains respectively, where n_{sd} is the number of space dimensions, and let Γ denote the boundary of Ω. The Navier-Stokes equations governing incompressible fluid flow are given as:

$$\rho(\frac{\partial \mathbf{u}}{\partial t} + \mathbf{u}\cdot\nabla\mathbf{u}) - \nabla\cdot\boldsymbol{\sigma} = \mathbf{0}, \qquad \nabla\cdot\mathbf{u} = 0 \qquad \text{on } \Omega \text{ for } (0,T). \tag{1}$$

Here ρ, $\mathbf{u}$ and $\boldsymbol{\sigma}$ are the density, velocity and the stress tensor, respectively. The stress tensor is represented as $\boldsymbol{\sigma} = -p\mathbf{I} + \mu((\nabla\mathbf{u}) + (\nabla\mathbf{u})^T)$, where p and μ are the pressure and coefficient of dynamic viscosity, respectively. The boundary conditions are specified as:

$$\mathbf{u} = \mathbf{g} \quad \text{on } \Gamma_g, \qquad \mathbf{n} \cdot \sigma = \mathbf{h} \quad \text{on } \Gamma_h \tag{2}$$

Here, Γ_g and Γ_h are the complementary subsets of the boundary Γ where Dirichlet and Neumann boundary conditions are specified, respectively.

To understand the evolution of small disturbances, the unsteady solution is expressed as a combination of steady solution and disturbance:

$$\mathbf{u} = \mathbf{U} + \mathbf{u}', \qquad p = P + p' \tag{3}$$

Here, $\mathbf{U}$ and P represent the steady state solution whose stability is to be determined while $\mathbf{u}'$ and p' are the perturbation fields. Substituting the decomposition given by Eq. (3) in Eqs. (1) and subtracting from them, the equations for steady flow one obtains the evolution equations for the disturbance fields. Further, the perturbations, $\mathbf{u}'$ and p', are assumed to be small and the non-linear terms are dropped. The linearized perturbation equations are given as:

$$\rho\left(\frac{\partial \mathbf{u}'}{\partial t} + \mathbf{u}' \cdot \nabla \mathbf{U} + \mathbf{U} \cdot \nabla \mathbf{u}'\right) - \nabla \cdot \boldsymbol{\sigma}' = \mathbf{0}, \qquad \nabla \cdot \mathbf{u}' = 0 \qquad \text{on } \Omega \text{ for } (0,T). \tag{4}$$

Here, $\boldsymbol{\sigma}'$ is the stress tensor for the perturbed solution. Eq. (4) subjected to the initial condition, $\mathbf{u}'(\mathbf{x},0) = \mathbf{u}'_0$ describes the evolution of small disturbances in the domain, Ω. The boundary conditions on $\mathbf{u}'$ are homogeneous versions of those used for calculating the base flow (Eq. (2)).

2.2 Global Linear Stability Analysis

To conduct a global Linear stability analysis we assume the following form of the disturbance field, $\mathbf{u}'$ and p'

$$\mathbf{u}'(\mathbf{x},t) = \hat{\mathbf{u}}(\mathbf{x})e^{\lambda t}, \qquad p'(\mathbf{x},t) = \hat{p}(\mathbf{x})e^{\lambda t} \tag{5}$$

Substituting Eqs. (5) in the linearized disturbance equations (Eqs. (4)) we obtain:

$$\rho(\lambda \hat{\mathbf{u}} + \hat{\mathbf{u}} \cdot \nabla \mathbf{U} + \mathbf{U} \cdot \nabla \hat{\mathbf{u}}) - \nabla \cdot \hat{\boldsymbol{\sigma}} = \mathbf{0}, \qquad \nabla \cdot \hat{\mathbf{u}} = 0 \qquad \text{on } \Omega. \tag{6}$$

Eqs. (6) represents a generalized eigenvalue problem with λ as the eigenvalue and $(\hat{\mathbf{u}}, \hat{p})$ as the corresponding eigenmode. The boundary conditions for $(\hat{\mathbf{u}}, \hat{p})$ are homogeneous version of those used for calculating the base flow $(\mathbf{U}, P)$. In general, the eigenvalue $\lambda = \lambda_r + i\lambda_i$ is complex. The growth rate is given by the real part, λ_r of the eigenvalue whereas the imaginary part, λ_i is related to the temporal frequency of the of the disturbance field. A positive value of λ_r indicates an unstable mode. This method has been utilized by several researchers in the past to investigate the global linear stability of various steady flow configurations [Jackson (1987); Morzynski and Thiele (1991); Morzynski, Afanasiev, and Thiele (1999); Swaminathan, Sahu, Sameen, and Govindrajan (2011)]. Mittal and Kumar (2003) proposed a stabilized finite element formulation for solving these equations and employed it to study the global stability properties of the flow past a stationary and rotating cylinder.

2.3 Local Stability Analysis: Orr-Sommerfeld Equation

Let (u', v', w') represent the general perturbation field with respect to the parallel base flow $(U(y), 0, 0)$. The linearized disturbance equation described by Eq. (4) can be simplified as:

$$[(\frac{\partial}{\partial t} + U\frac{\partial}{\partial x})\nabla^2 - \frac{\partial^2 U}{\partial y^2}\frac{\partial}{\partial x} - \frac{1}{Re}\nabla^4]v' = 0. \tag{7}$$

The disturbance field is assumed to be periodic along the two homogeneous directions: x and z. The wavenumbers along the x and z directions are α and β, respectively. Thus, the perturbation field in this scenario is given by:

$$v' = \hat{v}(y)e^{i(\alpha x + \beta z)}e^{\lambda t}. \tag{8}$$

Similar expressions can be written for u' and w', which represent the x and z component of the disturbance field. Let, $\mathbf{k} = \alpha\hat{i} + \beta\hat{k}$ represent the wavenumber vector in the $x - z$ plane with its magnitude given by $k = \sqrt{\alpha^2 + \beta^2}$. Substituting, Eq. (8) in the linearized disturbance equation described by Eq. (7), we obtain:

$$[\frac{1}{\alpha Re}(D^2 - k^2)^2 - iU(D^2 - k^2) + i\frac{\partial^2 U}{\partial y^2}]\hat{v} = \frac{\lambda}{\alpha}[D^2 - k^2]\hat{v}. \tag{9}$$

Here, D denotes $\frac{\partial}{\partial y}$. Further, it can be shown that for a parallel flow the two dimensional perturbations posses the largest growth rate [Schmid and Henningson (2001)]. Therefore, we confine the discussions in the rest of the article to two-dimensional disturbances. For a $2 - D$ disturbance, Eq. (8) can be simplified to:

$$v' = \hat{v}(y)e^{i\alpha x}e^{\lambda t}. \tag{10}$$

We consider the case when the streamwise wavenumber, α, is real and the eigenvalue $\lambda = \lambda_r + i\lambda_i$ is complex. The real part, λ_r, is the growth rate of the disturbance while λ_i, the imaginary part, is the temporal frequency of the disturbance. The disturbance associated with the eigenvalue that has the largest real mode is of major interest as it represents the fastest growing mode. For $2-D$ disturbances we can rewrite Eq. (9) to obtain the Orr-Sommerfeld (OS) equation:

$$[\frac{1}{Re}(D^2-\alpha^2)^2 - i\alpha U(D^2-\alpha^2) \qquad + i\alpha\frac{\partial^2 U}{\partial y^2}]\hat{v} = \lambda[D^2-\alpha^2]\hat{v}. \tag{11}$$

The disturbance velocity, u', v' must vanish on the far-field and solid boundaries, Γ. For the periodic disturbance field considered this requires $\hat{u}, \hat{v}$ to vanish on Γ. Using the continuity equation, one can simplify this to:

$$\hat{v} = 0, \qquad \frac{d\hat{v}}{dy} = 0 \qquad \text{on } \Gamma. \tag{12}$$

3 Formulation

3.1 The Stabilized Finite Element Formulation for Global Linear Stability Analysis

Let $\Omega \subset \mathbb{R}^2$ be the spatial domain for global linear stability analysis (Eq. (6)). Consider a finite element discretization of Ω into subdomains $\Omega^e, e = 1,2,3,...,n_{el}$, where n_{el} is the number of elements. Based on this discretization we define finite element trial function spaces for velocity and pressure perturbation fields as $\mathscr{S}^h_{\mathbf{u}}$ and $\mathscr{S}^h_p$, respectively. The weighting function space are $\mathscr{V}^h_{\mathbf{u}}$ and $\mathscr{V}^h_p$, respectively. These function spaces are selected by taking the homogeneous Dirichlet boundary conditions into account, as subsets of $[H^{1h}(\Omega)]^2$ and $H^{1h}(\Omega)$, where $H^{1h}(\Omega)$ is the finite dimensional function space over Ω. The stabilized finite element formulation of Eq. (6), is as follows: Find $\hat{\mathbf{u}}^h \in \mathscr{S}^h_{\mathbf{u}}$ and $\hat{p}^h \in \mathscr{S}^h_p$ such that $\forall \hat{\mathbf{w}}^h \in \mathscr{V}^h_{\mathbf{u}}$ and $\hat{q}^h \in \mathscr{V}^h_p$

$$\begin{aligned}
&\int_\Omega \hat{\mathbf{w}}^h \cdot \rho \left(\lambda \hat{\mathbf{u}}^h + \mathbf{U}^h \cdot \boldsymbol{\nabla}\hat{\mathbf{u}}^h + \hat{\mathbf{u}}^h \cdot \boldsymbol{\nabla}\mathbf{U}^h\right) d\Omega + \int_\Omega \boldsymbol{\varepsilon}(\hat{\mathbf{w}}^h) : \boldsymbol{\sigma}(\hat{p}^h, \hat{\mathbf{u}}^h) d\Omega \\
&\quad + \int_\Omega \hat{q}^h \boldsymbol{\nabla} \cdot \hat{\mathbf{u}}^h d\Omega + \sum_{e=1}^{n_{el}} \int_{\Omega^e} \frac{1}{\rho}\left(\tau_{\text{SUPG}}\rho \mathbf{U}^h \cdot \boldsymbol{\nabla}\hat{\mathbf{w}}^h + \tau_{\text{PSPG}} \boldsymbol{\nabla}\hat{q}^h\right) \cdot \\
&\quad \left[\rho \left(\lambda \hat{\mathbf{u}}^h + \mathbf{U}^h \cdot \boldsymbol{\nabla}\hat{\mathbf{u}}^h + \hat{\mathbf{u}}^h \cdot \boldsymbol{\nabla}\mathbf{U}^h\right) - \boldsymbol{\nabla} \cdot \boldsymbol{\sigma}(\hat{p}^h, \hat{\mathbf{u}}^h)\right] d\Omega^e \\
&\quad + \sum_{e=1}^{n_{el}} \int_{\Omega^e} \tau_{\text{LSIC}} \boldsymbol{\nabla} \cdot \hat{\mathbf{w}}^h \rho \boldsymbol{\nabla} \cdot \hat{\mathbf{u}}^h d\Omega^e = 0.
\end{aligned} \tag{13}$$

Here, $\mathbf{U}^h$ represents the base flow at the element nodes. In the variational formulation given by Eq. (13), the first three terms constitute the Galerkin formulation of the problem. The terms involving the element level integrals are the stabilization terms added to the basic Galerkin formulation to enhance its numerical stability. These terms stabilize the computations against node-to-node oscillations in advection dominated flows and allow the use of equal-in-order basis functions for velocity and pressure. The terms with coefficients τ_{SUPG} and τ_{PSPG} are based on the SUPG (Streamline-Upwind/Petrov-Galerkin) [Brooks and Hughes (1982)] and PSPG (Pressure-stabilized/Petrov-Galerkin) [Tezduyar, Mittal, Ray, and Shih (1992)] stabilizations. The SUPG formulation for convection dominated flows was introduced by Hughes and Brooks (1979) and Brooks and Hughes (1982). PSPG stabilization for enabling the use of equal-order interpolations for the velocity and pressure to fluid flows at finite Reynolds number was introduced by Tezduyar, Mittal, Ray, and Shih (1992). The term with coefficient τ_{LSIC} is a stabilization term based on the least squares of the divergence free condition on the velocity field. It provides numerical stability at high Reynolds number. Here, the stabilization coefficients used in the finite element formulation of LSA (Eq. (13)) are computed on the basis of the base flow at the element nodes, $\mathbf{U}^h$. The stabilization parameters are defined as [Tezduyar, Mittal, Ray, and Shih (1992)]:

$$\tau_{LSIC} = \left[\left(\frac{2}{h^e ||\boldsymbol{U}^h||} \right)^2 + \left(\frac{12\nu}{(h^e)^2 ||\boldsymbol{U}^h||^2} \right)^2 \right]^{-1/2}, \tag{14}$$

$$\tau_{SUPG} = \tau_{PSPG} = \left[\left(\frac{2||\boldsymbol{U}^h||}{h^e} \right)^2 + \left(\frac{12\nu}{(h^e)^2} \right)^2 \right]^{-1/2}, \tag{15}$$

Here, h^e is the element length based on the minimum edge length of an element [Mittal (2000)] and $\mathbf{U}^h$ is the base flow velocity at element nodes.

Eq. (13) lead to a generalized non-symmetric eigenvalue problem of the form $\mathbf{A}X - \lambda \mathbf{B}X = 0$. For our case, the eigenvalue problem is slightly more complicated as the continuity equation responsible for determining pressure causes the matrix $\mathbf{B}$ to become singular. Hence, to avoid singularity, we solve the inverse problem, i.e., eigenvalues for $\mathbf{B}X - \mu \mathbf{A}X = 0$ are computed. Here, $\lambda = 1/\mu$. To check the stability of the steady-state solution we look for the rightmost eigenvalue (eigenvalue with largest real part), using the subspace iteration method [Stewart (1975)].

3.2 The Spectral Method for Local Linear Stability Analysis

The spectral collocation method based on Chebyshev polynomials of the first kind [Schmid and Henningson (2001)] is used to solve the Eq. (11) for carrying out the local stability analysis. The Chebyshev polynomial of the first kind is defined as:

$$T_n(y) = cos(n\, cos^{-1}(y)) \tag{16}$$

for all non-negative integers $n \in [0, N]$ and $y \in [-1, 1]$. By using a suitable transformation, it is possible to map any other range of y to the Chebyshev domain $[-1, 1]$. The Chebyshev polynomials are utilized as the basis functions to approximate the eigenfunction, $\hat{v}(y)$ in Eq.(8):

$$\hat{v}(y) = \sum_{n=0}^{N} a_n T_n(y). \tag{17}$$

This approximation of the eigenfunction is substituted in the OS equation (Eq.(11). It results in the following equation:

$$\begin{aligned}
&\frac{1}{Re}\Big(\sum_{n=0}^{N} a_n T_n^{''''}(y) - 2\alpha^2 \sum_{n=0}^{N} a_n T_n^{''}(y) + \alpha^4 \sum_{n=0}^{N} a_n T_n(y)\Big) + \\
&-i\alpha[U(\sum_{n=0}^{N} a_n T_n^{''}(y) - \alpha^2 \sum_{n=0}^{N} a_n T_n(y)) - U_{yy} \sum_{n=0}^{N} a_n T_n(y)] \\
&\qquad\qquad = \lambda[\sum_{n=0}^{N} a_n T_n^{''}(y) - \alpha^2 \sum_{n=0}^{N} a_n T_n(y)].
\end{aligned} \tag{18}$$

The collocation method is employed to evaluate the constants a_n in the approximation given by Eq. (17). The following Gauss-Lobatto collocation points are used:

$$y_j = cos(\frac{j\pi}{N}) \qquad j = 0, 1, 2, 3, ..., N. \tag{19}$$

Eq. (18) leads to the generalized eigenvalue problem of the form $\mathbf{A}X - \lambda \mathbf{B}X = 0$. In the present work, the numerical solution to the same is obtained using LAPACK [Anderson, Bai, Bischof, Blackford, Demmel, Dongarra, Du Croz, Greenbaum, Hammarling, McKenney, and Sorensen (1999)] libraries.

4 Problem Setup

4.1 The Base Flow

The local and the global linear stability analysis are carried out for the plane Poiseuille flow. Figure (1) shows the schematic of the flow. The fluid occupies the channel formed by two stationary plates parallel to each other and separated by a distance $2H$. The plates are aligned with the $x-$ axis. The velocity profile for the base flow

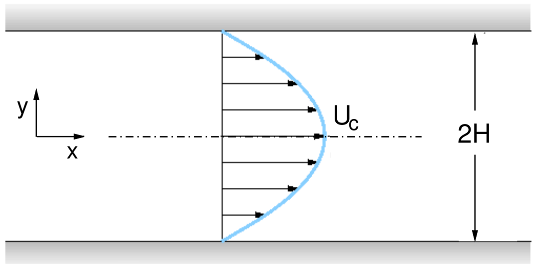

Figure 1: Schematic of the plane Poiseuille flow.

is shown in the figure. It is parabolic and symmetric about the channel centerline. The equation for the streamwise component of velocity is given as:

$$U = U_c\big(1 - (\frac{y}{H})^2\big). \tag{20}$$

Here, H denotes half the channel width and U_c is the centerline velocity. All the lengths are non-dimensionalized with H, and velocity with U_c. The Reynolds number, Re, is defined as:

$$Re = \frac{U_c H}{\nu}, \tag{21}$$

where, ν denotes the kinematic viscosity of the fluid.

4.2 Local Linear Stability Analysis

The local analysis of the plane Poiseuille flow is carried out via the solution to OS (Eq. (11)). The domain across the channel width, $[-H,H]$, is mapped to $[-1,1]$. No-slip boundary conditions are applied to the disturbance field at the channel walls. In this situation, Eq. (12) can be rewritten as:

$$\hat{v}(y = \pm H) = 0, \qquad \frac{d\hat{v}}{dy}(y = \pm H) = 0. \tag{22}$$

The OS equation (Eq. (11)), along with the boundary conditions (Eq. (22), is solved in the temporal point of view. The wavenumber, α, is assumed to be real. The OS equation is solved for different values of values of α and Re. The effect of the number of grid points, along y, on the accuracy of the solution is investigated. It is found that 200 collocation points provide adequate spatial resolution. All the results presented in this paper for the OS analysis are with 200 points.

4.3 Global Linear Stability Analysis

The flow in a finite streamwise length of the channel (=L) is considered for carrying out the global analysis. The base flow is the fully developed steady flow in the channel. The streamwise velocity for the same is given by Eq.(20). The boundary conditions for the disturbance field are as follows. The disturbance velocity is prescribed a zero value at the upper and lower walls. To enable comparison with the local analysis, the disturbance is assumed to be periodic in the streamwise direction. Therefore, periodic boundary conditions are applied on all the variables at the inflow and the outflow boundaries. The finite element mesh consists of 24 elements along the streamwise and 150 elements in the cross-flow directions. The grid points are uniformly spaced along x but are clustered close to the wall in the y direction. A mesh convergence study is carried out for the $Re = 7000$ plane Poiseuille flow and $L/2H = 1$. A more refined grid with roughly twice the resolution in each direction leads to less than one percent difference in the results, thereby reflecting the adequacy of the original finite element mesh.

5 Results: Linear Stability Analysis of the Plane Poiseuille Flow

5.1 OS Analysis

Local analysis via solution to the OS equation (Eq. (11)) is carried out for various values of Re and α. At each (Re, α) the eigenvalue with the largest real part is identified. Figure (2) shows the variation of the growth rate of the disturbance associated with the rightmost eigenvalue with Re and α. The figure shows the iso-contours for various values of growth rate in the $Re - \alpha$ plane. The contour corresponding to zero growth rate is the neutral curve. The critical Re for the onset of instability is the lowest value of the Re on the neutral curve, for any value of α. The critical Re for this flow is found to be 5773, approximately and is marked in Figure (2). The value is in excellent agreement with results from earlier studies [Schmid and Henningson (2001)].

The results for the flow at $Re = 7000$ are presented in more detail in Figure (3). This figure shows the variation of the real (λ_r) and imaginary (λ_i) parts of the rightmost eigenvalue with wavenumber (α) at $Re = 7000$. While λ_r denotes the growth rate, λ_i is related to the temporal frequency of the disturbance. We observe that the $Re = 7000$ flow is linearly unstable only to disturbances whose wavenumber lies in a specific interval. The maximum growth rate is 0.0017, approximately for $\alpha = 1.00$.

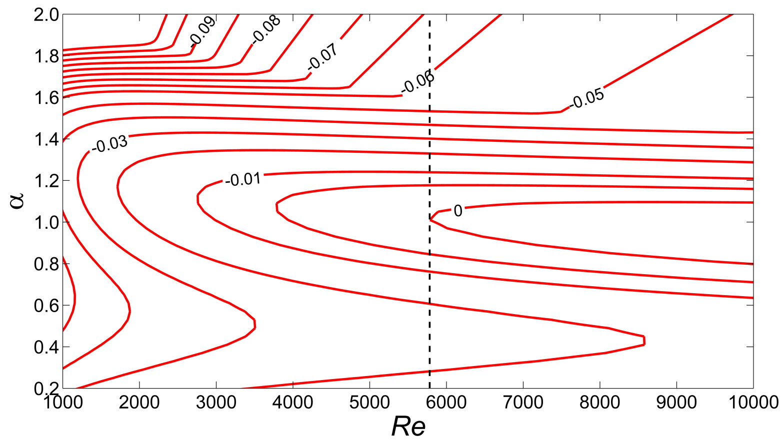

Figure 2: Orr-Sommerfeld analysis of the Plane Poiseuille flow: iso-contours of constant growth rate. The critical *Re* for the onset of the instability of the flow is $Re_{cr} = 5773$ and is marked with a vertical broken line.

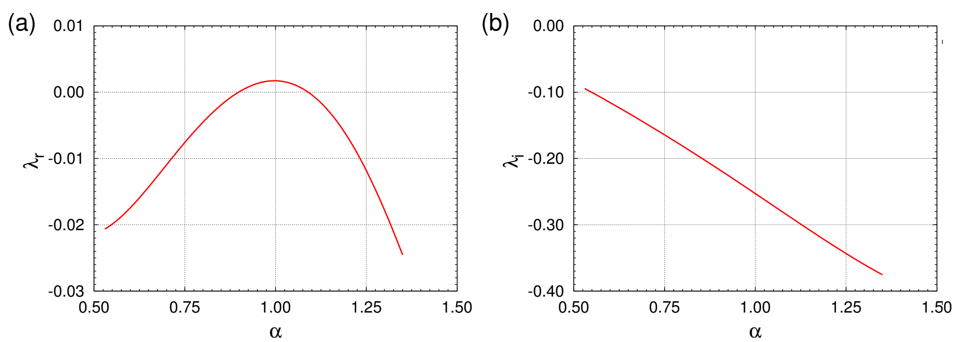

Figure 3: Orr-Sommerfeld Analysis of the Plane Poiseuille Flow at $Re = 7000$: variation of real and imaginary part of the right-most eigenvalue with wavenumber, α.

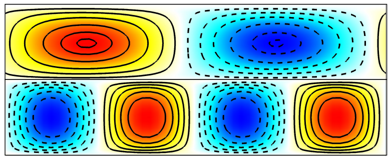

Figure 4: Global linear stability analysis of the Plane Poiseuille flow for $Re = 7000$ and $L/2H = 5.10$: the v' field for the eigenmodes corresponding to the two rightmost eigenvalues. The upper row corresponds to one cell in the domain ($n = 1$) and has a growth rate, $\lambda_r = -0.017$. The lower row is for $n = 2$ with two cells in the domain; the growth rate for this mode is $\lambda_r = -0.0097$.

5.2 Global Analysis

In the local analysis, the OS equation (Eq. (11)) can be solved by using α as one of the independent variables. However, the global analysis (Eq. (6)) does not directly offer α as an independent variable. The analysis, of course, can be carried out for different streamwise extent (L) of the computational domain. We attempt to understand the relation between L (for the global analysis) and α (for the local analysis). We propose that for a spatially periodic disturbance, its wavenumber is related to the length of the computational domain as:

$$\alpha = \frac{2\pi n}{L}, \tag{23}$$

where, n is the number of waves along the stream wise direction in the domain. To demonstrate this, we consider the global linear stability analysis for $Re = 7000$. Fig. (4) shows the eigen modes associated with the two right most eigenvalues for $L/2H = 5.1$. While the first one is associated with one wave ($n = 1$), the other houses two waves ($n = 2$) in the computational domain. Thus, they both represent different wave numbers and are associated with their own growth rates, as listed in the caption of the figure. The real and imaginary part of the eigenvalue obtained from the global analysis, and their comparison with the values obtained from the local analysis, are also shown in Figures (5) and (6). The data points corresponding to the two eigenmodes lie on the vertical line segment marked in the two figures for $L/2H = 5.10$. The values from the local and global analysis are in excellent agreement.

Figures (5) and (6) show the variation of the growth rate and the imaginary part of the rightmost eigenvalue from the global analysis for plane Poiseuille flow at $Re = 7000$. The data points from the global analysis are marked by solid circles. Also shown in the same figure are the results from the local analysis. The variation is associated with a number of peaks and valleys. We attempt to understand this behavior. It is demonstrated in Fig. (4) that the computational domain may accommodate multiple cells of the disturbance. We first identify in Figs. (5) and (6) the cases that are associated with one cell only ($n = 1$) in the streamwise extent of the domain. A best fit to these points is in excellent agreement with the results from the local analysis. These curves are marked as $L = 2\pi/\alpha$ in the figures. These curves can also be utilized to understand the variation of λ_r and λ_i with α. We note that the growth rate and temporal frequency of an eigenmode should depend on α, but must be independent of the number of cells of the same α in the computational domain. Using this idea, and the data for λ_r and λ_i v/s α from the local analysis, the variation of λ_r and λ_i with $L/2H$ is generated for multiple cells by observing that $L = 2\pi n/\alpha$, where n is the number of cells. These curves are shown in Figs. (5) and (6) for various values of n. The outer envelope of these curves is shown in thicker solid line. These curves provide an estimate of the variation of the rightmost eigenvalue with the length of the computational domain. Excellent agreement is observed between the estimated rightmost eigenvalue and the actual value from global LSA computations for $n \geq 2$. We note that as the length of the computational domain is increased, the dependence of the growth rate of the most unstable eigenmode on L becomes weaker. In the asymptotic limit of the domain being infinitely long, the fastest growing mode comprises of infinite cells of the $n = 1$ eigenmode whose wavenumber is associated with largest λ_r. We also note from Fig. (5) that in certain situations it might be difficult to track the eigenmodes corresponding to low values of α from the global analysis. Low values of α correspond to large $L/2H$. As seen from Fig. (5), at large $L/2H$, $n = 1$ mode is not necessarily the one with rightmost eigenvalue. For example, at $L/2H = 15$ the rightmost eigenvalue corresponds to the mode with five cells ($n = 5$). The modes with four, three, two and one cell have lower growth rate, and in the same order. Therefore, tracking the mode for $n = 1$ for this value of $L/2H$ is relatively more challenging than the ones for higher values of n.

To further demonstrate that the growth rate and temporal frequency of an eigenmode must be independent of the number of streamwise cells in the global analysis, we consider the case where we seek the rightmost eigenvalue for $\alpha = 1.05$. For $n = 1$, this corresponds to $L/2H = 3.0$, approximately. Figure (7) shows the eigenmodes from the global analysis for various values of $L/2H$ for the same α ($= 1.05$). The various values of L are chosen by varying n in the relation $L = 2\,n\,\pi/\alpha$. A broken horizontal line is marked in Figures (5) and (6) to show the real and imaginary part of the rightmost eigenvalue for various values of L that correspond to $\alpha = 1.05$. We observe that all these modes are associated with the same eigenvalue. In fact, the eigenmodes are also of the same family. They are shown in Figure (7) and have

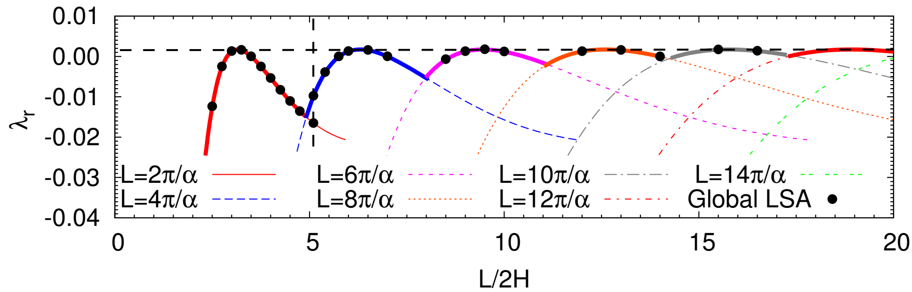

Figure 5: Variation of the growth rate of the leading eigenvalue with $L/2H$ for the plane Poiseuille flow for $Re = 7000$: the solid dots represent the growth rate of the most unstable mode obtained at various values of $L/2H$ from global LSA. The solid (red) curve is obtained from the local (Orr-Sommerfeld) analysis. It is in excellent agreement with the best fit to the points corresponding to one streamwise wave ($n = 1$) from global analysis as per the relation $L = 2\pi/\alpha$. The curve is replicated for various n to show the predicted variation of λ_r with L, for the global analysis using the relation $L = n(2\pi/\alpha)$, when the domain houses different number of cells. The outer envelope of these curves, shown in thicker solid line, represents the eigenmode associated with the rightmost eigenvalue for the corresponding length of the computational domain.

the same flow structure, albeit with different number of cells.

6 Concluding Remarks

Hydrodynamic stability of shear flows has been widely investigated in the past using local and global Linear Stability Analysis (LSA). In this work we have reviewed the two approaches and attempted to highlight the difference between the two in the context of their application to parallel shear flows. Results for the linear stability of plane Poiseuille flow have been presented, using both approaches. The local analysis is carried out by solving the Orr-Sommerfeld (OS) equation using the spectral collocation method based on Chebyshev polynomials. The analysis has been carried out for various wavenumbers, α of the streamwise periodic disturbance field. The critical Re for the onset of linear instability for plane Poiseuille flow is found to be 5773, which is in good agreement with earlier results [Schmid and Henningson (2001)]. The stability of the flow at $Re = 7000$ has been presented in more detail. For example, the variation of the real and imaginary part of the least stable eigenvalue with α has been presented. Unlike the local analysis which involves

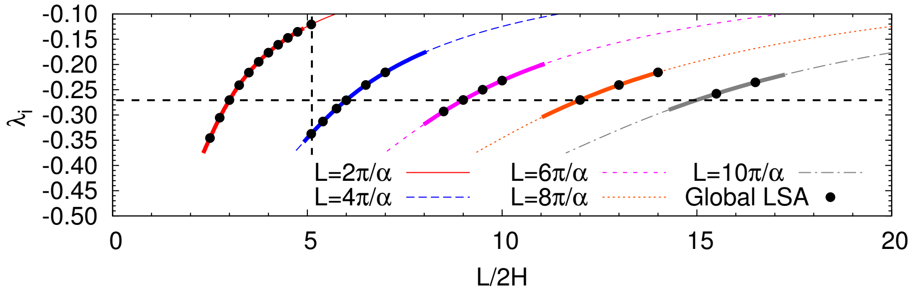

Figure 6: Variation of the imaginary part of the leading eigenvalue with $L/2H$ for the plane Poiseuille flow for $Re = 7000$: the solid dots represent the imaginary part of the most unstable mode obtained at various values of $L/2H$ from global LSA. The solid (red) curve is obtained from the local (Orr-Sommerfeld) analysis. It is in excellent agreement with the best fit to the points corresponding to one streamwise wave ($n = 1$) from global analysis as per the relation $L = 2\pi/\alpha$. The curve is replicated for various n to show the predicted variation of λ_i with L, for the global analysis using the relation $L = n(2\pi/\alpha)$, when the domain houses different number of cells. The curves shown in thicker solid line represents λ_i associated with the rightmost eigenvalue for the corresponding length of the computational domain.

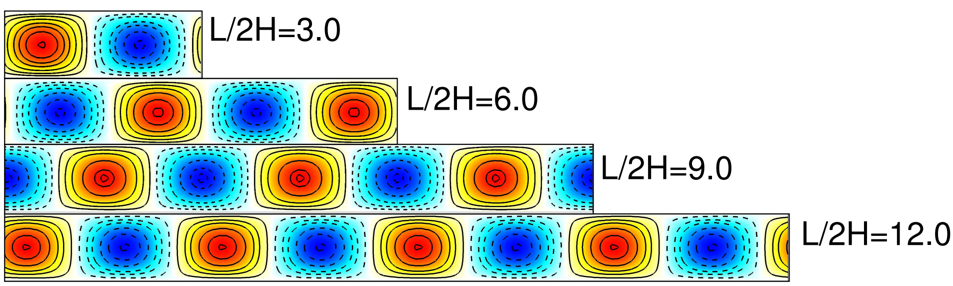

Figure 7: Eigenmodes of v' corresponding to the leading eigenvalue for various lengths of the domain obtained with the global LSA for the plane Poiseuille flow for $Re = 7000$ for disturbances that are periodic in the streamwise direction.

solution to an ordinary differential equation, the global analysis involves finding solution to a set of partial differential equations. The analysis has been carried out for a two-dimensional disturbance field that is assumed to be spatially periodic along the stream wise direction. A stabilized finite element method has been presented for carrying out the global LSA in primitive variables. Equal-in-order finite element functions are used for representing velocity and pressure. To suppress the numerical oscillations that might appear in the computations, the SUPG and PSPG, stabilizations are added to the Galerkin finite element formulation. The formulation has been used to carry out the linear stability analysis for the plane Poiseuille flow at $Re = 7000$. Computations are carried out for various values of the streamwise length, L, of the computational domain.

Unlike the local analysis, the global analysis can handle non-periodic disturbances and is applicable to non-parallel flows as well. However, the global analysis is significantly more expensive than the local analysis. For the parallel flow and with spatially periodic disturbances the present work brings out a very interesting relationship between the wave number of the disturbance and the streamwise extent of the domain in the global analysis. When the eigenmode contains only once cell, the results from the local and global analysis are virtually identical; the wavenumber and streamwise extent of the domain are related as $\alpha = 2\,\pi/L$. However, when the eigenmode consists of n cells along the streamwise length of the domain the relationship is: $\alpha = (2\,\pi n)/L$. For a very large value of L, the global analysis results in an eigenmode with a large number of cells of the eigenmode whose α corresponds to the mode with largest growth rate. If one would like to use the global analysis to create the growth rate v/s α curve for the rightmost eigenvalue, as is done in the local analysis for a specific value of Re, the procedure is complicated by the number of cells that are housed in the domain. In the scenario when L is relatively large, to track an eigenmode for low α, the eigenmode associated with one cell might not be the most unstable mode. Therefore, one needs to examine the eigenmodes for the first few eigenvalues that are arranged in the descending order of their real part. The one that corresponds to $\alpha = 2\,\pi/L$ is the eigenmode which consists of only one cell along the streamwise direction.

Acknowledgement: The help from Mr. Hardik Parwana in carrying out some of the computations is gratefully acknowledged.

References

Anderson, E.; Bai, Z.; Bischof, C. et al. (1999): *LAPACK Users' Guide*. Society for Industrial and Applied Mathematics, Philadelphia, PA, third edition.

Boiko, A. V.; Dovgal, A. V.; Grek, G. R. et al.(2012): *Physics of Transitional Shear Flows*. Springer-Verlag.

Brooks, A.; Hughes, T. (1982): Streamline upwind/petrov-galerkin formulations for convection dominated flows with particular emphasis on the incompressible navier-stokes equations. *Computer Methods in Applied Mechanics and Engineering*, vol. 32, pp. 199-259.

Chandrasekhar, S. (1981): Hydrodynamic and hydromagnetic stability. Dover.

Chomaz, J.-M. (2005): Global instabilities in spatially developing flows: non-normality and nonlinearity. *Annual Review of Fluid Mech.*, vol. 37, pp. 357-392.

Chomaz, J. M.; Huerre, P.; Redekopp, L. G. (1988): Bifurcations to local and global modes in spatially developing flows. *Physical Review Letters*, vol. 60, pp. 25-28.

Davey, A.; Drazin, P. (1969): The stability of poiseuille flow in a p ipe. *J. Fluid Mech.*, vol. 36, pp. 209-218.

Garg, V. K.; Rouleau, W. T. (1972): Linear spatial stability of pipe poiseuille flow. *J. Fluid Mech.*, vol. 54, pp. 113-127.

Gaster, M. (1962): A note on the relation between temporally-increasing and spatially-increasing disturbances in hydrodynamic stability. *J. Fluid Mech.*, vol. 14, pp. 222-224.

Huerre, P. (2000): Open shear flow instabilities. In Batchelor, G .; Moffatt, H.; Worster, M.(Eds): Perspectives in Fluid Dynamics, pp. 159-229. Cambridge.

Huerre, P.; Monkewitz, P. (1990): Local and global instabilities in spatially developing flows. *Annual Review of Fluid Mech.*, vol. 22, pp. 473-537.

Hughes, T.; Brooks, A. (1979): A multi-dimensional upwind scheme with no crosswind diffusion. *Journal of Applied Mechanics*, vol. 34, pp. 19-35.

Jackson, C. (1987): A finite element study of the onset of vortex shedding in flow past variously shaped bodies. *J. Fluid Mech.*, vol. 182, pp. 23.

Jackson, C. (1987): A finite element study of the onset of vortex shedding in flow past variously shaped bodies. *J. Fluid Mech.*, vol. 182, pp. 23.

Mittal, S. (2000): On the performance of high aspect-ratio elements for incompressible flows. *Computer Methods in Applied Mechanics and Engineering*, vol.

188, pp. 269-287.

Mittal, S. (2004): Three-dimensional instabilities in flow past a rotating cylinder. *Journal of Applied Mechanics*, vol. 71, pp. 89-95.

Monkewitz, P. A. (1988): The absolute and convective nature of instability in two-dimensional wakes at low oeynolds numbers. *Physics of Fluids*, vol. 31, pp.999-1006.

Morzynski, M.; AÑanasiev, K.; Thiele, c. (1999): Solution of the eigenvalue problems resulting from global non-parallel flow stability analysis. *Comput. Methods Appl. Mech. Eng.*, vol. 169, pp. 161.

Morzynski, M.; Thiele, c. (1991): kumerical stability analysis of a flow about a cylinder. Z. Angew. *Math. Mech.*, vol. 71, pp. T424.

Navrose; Meena, J.; Mittal, S. (2015): Three-dimensional flow past a rotating cylinder. *J. Fluid Mech.*, vol. 766, pp. 28-53.

Orr, W. M. (1907): The stability or instability of the steady motions of a perfect liquid and of a viscous liquid. Proc. o. *I rish Acad. Sec*. A, vol. 27, pp. 9-138.

Orszag, S. A. (1971): Accurate solution of the orr-sommerfeld stability equation. *J. Fluid Mech.*, vol. 50, pp. 689-703.

Pierrehumbert, R. T. (1985): Local and global baroclinic instability of zonally varying flow. *Journal of the Atmospheric Sciences*, vol. 41, pp. 2141-2162.

Saraph, V.; Vasudeva, B. R.; Panikar, J. (1979):Stability of parallel flows by the finite element m ethod. *Int. J. Numer. Methods Engineering*, vol. 17, pp. 853-870.

Schmid, P. J.; Henningson, D. S. (2001): *Stability and Transition in Shear Flows*. Springer-Verlag.

Sommerfeld, A. (1908): Ein Beitrag zur hydrodynamischen Erkläerung der turbulenten Flüessigkeitsbewegungen. *Proc. Fourth Internat. Cong. Math.*, Rome, vol. III, pp. 116-128.

Stewart, G. (1975): Methods of simultaneous iteration for calculating eigenvectors of matrices. *In Miller, J.(Ed): Topics in Numerical Analysis II*, pp. 169-185. Academic Press: New York.

Swaminathan, G.; Sahu.; Sameen, A.; Govindrajan, R. (2011): Global instabilities in diverging channel flows. *Theor. Comput. Fluid Dyn.*, vol. 25, pp. 5-64.

Tezduyar, T.; Mittal, S.; Ray, S.; Shih, R. (1992): Incompressible flow computations with stabilized bilinear and linear equal-order-interpolation velocity-pressure elements. *Comput. Meth. Appl. Mech. Engrg*, vol. 95, pp. 221.

Theofilis, V. (2011): Global linear i nstability. *Annual Review of Fluid Mech.*, vol. 43, pp. 319-352.

Verma, A.; Mittal, S. (2011): A new unstable mode in the wake of a circular cylinder. *Phys. Fluids.*, vol. 23, pp. 121701.

Yang, X.; Zebib, A. (1989): Absolute and convective instability of a cylinder wake. *Physics of Fluids A*, vol. 1, pp. 689-696.